Published in final edited form as:
Eur J Immunol. 2012 June ; 42(6): 1500–1511. doi:10.1002/eji.201142051.

Caveolin-1 plays a critical role in host immunity against *Klebsiella pneumoniae* by regulating STAT5 and Akt activity

Qiang Guo[1,2], **Nan Shen**[2], **Kefei Yuan**[1], **Jiaxin Li**[1,3], **Hong Wu**[3], **Yong Zeng**[3], **John Fox III**[1], **Arvind K. Bansal**[4], **Brij B. Singh**[1], **Hongwei Gao**[5], and **Min Wu**[1]

[1]Department of Biochemistry and Molecular Biology, University of North Dakota, Grand Forks, North Dakota, USA

[2]Department of Rheumatology Renji Hospital, Shanghai Jiaotong University, Shanghai, China

[3]Department of Hepatobiliary and Pancreatic Surgery West China Hospital, Sichuan University, Chengdu, China

[4]Pulmonary, Critical Care and Sleep Medicine, the Altru Hospital, Grand Forks, North Dakota, USA

[5]Center for Experimental Therapeutics and Reperfusion Injury, Department of Anesthesiology, Perioperative and Pain Medicine, Brigham and Women's Hospital, Harvard Medical School, Boston, Massachusetts, USA

Abstract

Caveolin-1 (Cav1) is a structural protein of caveolae. Although Cav1 is associated with certain bacterial infections, it is unknown whether Cav1 is involved in host immunity against *Klebsiella pneumoniae*, the third most commonly isolated microorganism from bacterial sepsis patients. Here, we showed that *cav1* knockout mice succumbed to *K. pneumoniae* infection with markedly decreased survival rates, increased bacterial burdens, intensified tissue injury, hyperactive proinflammatory cytokines, and systemic bacterial dissemination as compared with WT mice. Knocking down Cav1 by a dominant negative approach in lung epithelial MLE-12 cells resulted in similar outcomes (decreased bacterial clearance and increased proinflammatory cytokine production). Furthermore, we revealed that STAT5 influences the GSK3β–β-catenin–Akt pathway, which contributes to the intensive inflammatory response and rapid infection dissemination seen in Cav1 deficiency. Collectively, our findings indicate that Cav1 may offer resistance to *K. pneumoniae* infection, by affecting both systemic and local production of proinflammatory cytokines via the actions of STAT5 and the GSK3β–β-catenin–Akt pathway.

Keywords

Alveolar macrophage phagocytosis; Cell signaling pathway; Gram-negative bacterial infection; Innate immunity; Proinflammatory cytokines

Full correspondence: Prof. Min Wu, Department of Biochemistry and Molecular Biology, University of North Dakota, Grand Forks, ND 58203, USA Fax: +1-701-777-2382 min.wu@med.und.edu. ***Additional correspondence:*** Dr. Hongwei Gao, Center for Experimental Therapeutics and Reperfusion Injury, Department of Anesthesiology, Perioperative & Pain Medicine, Brigham and Women's Hospital, Harvard Medical School, Boston, MA 02201, USA Fax: +1-617-5255027 hgao@zeus.bwh.harvard.edu.

Supporting Information available online

Conflict of interest: The authors declare that they have no competing financial interests.

Introduction

Caveolae are flask-shaped lipid microdomains in the plasma membrane. As part of an alternative pathway to receptor-mediated endocytosis, caveolae are involved in various cellular activities such as lipid storage, phagocytosis, small molecule uptake, and secretion [1]. A recent addition to this list is a potential role in pathogenic infections. *Escherichia coli*, for example, relies on caveolae to invade both phagocytic and nonphagocytic cells [2].

Caveolae are composed of lipids and proteins. A major scaffold protein for these structures is Caveolin-1 (Cav1), which is expressed at high levels in endothelial and epithelial cells. Cav1 has been shown to be biologically important, having been shown to be involved in uptake of the Simian Virus-40 [3] and the BK virus [4]. Wang et al. [5] also demonstrated that Cav1 inhibits HIV-1 envelope-induced apoptosis through interactions with gp41 in $CD4^+$ T lymphocytes. Furthermore, Cav1 is involved in uptake of not only viral pathogens but also larger bacterial pathogens [6].

Knockout (KO) mouse studies have revealed multi-faceted roles for Cav1 in infectious diseases [7]. Malik et al. [7] found that *cav1* KO mice exhibited decreased mortality due to decreased levels of inflammation mediated by interactions with nitric oxide. In contrast, *cav1* KO mice with *Salmonella typhimurium* infection showed increased inflammatory cytokine levels and mortality [8]. Gadjeva et al. [9] showed that Cav1 is essential for host defense against *Pseudomonas aeruginosa* as *cav1* KO mice manifested a typical phenotype with decreased bacterial clearance and more severe infection. However, another study suggested that Cav1 is not involved in *P. aeruginosa* invasion in the lung [10]. Since there is so far no consensus on the function of Cav1 in various infections [11], further investigations are needed.

Here, we used a new murine model of *K. pneumoniae* infection to investigate the functions of Cav1 in host defense. *K. pneumoniae* is a capsulate gram-negative bacterium, and the third most commonly isolated microorganism in blood cultures from sepsis patients [12]. Due to emerging antibiotic resistance, *K. pneumoniae* infection remains a major health threat [13,14]. Therefore, a better understanding of its molecular pathogenesis is necessary. Here, we sought to define the host defenses generated against *K. pneumoniae* using *cav1* KO mice. We demonstrated that Cav1 deficiency led to a more severe disease phenotype in mice due to a dysregulated cytokine profile. Additionally, our results suggest that this phenotype depends on Akt-STAT5 cross-talk, involving the β-catenin–GSK3β signaling system.

Results

Cav1 regulates the susceptibility to acute pneumonia caused *by K. pneumoniae*

To determine the role of Cav1 in *K. pneumoniae* infection, we intranasally introduced this bacterium (2×10^5 CFU/mouse) to *cav1* KO and WT mice (with otherwise similar genetic backgrounds). We used KO mice within 4 months after birth as pulmonary abnormalities are known to occur after 6–12 months of age. This high inoculum was implemented to evaluate acute infection within 72 h [12,15]. As shown in Fig. 1A, the *cav1* KO mice rapidly succumbed to *K. pneumoniae* pneumonia with 66.7% mortality within 24 h and 100% mortality by 48 h. In contrast, the WT mice were profoundly resistant and showed significantly greater survival than the *cav1* KO group (Log-rank test, $p = 0.029$). These findings indicate that Cav1 significantly contributes to the resilience of these animals against *K. pneumoniae* infection.

Cav1 KO mice show elevated bacterial burdens in the lung

To compare the host responses to *K. pneumoniae* in *cav1* KO and WT mice, bacterial burdens in the lungs and other organs were determined. Animals were challenged with 2×10^5 CFU/mouse of *K. pneumoniae* and sacrificed at 24 h (5 mice/group). After BAL (bronchoalveolar lavage) procedures to remove free bacteria, the lungs were aseptically removed and homogenized in order to quantify bacterial burdens. C*av1* KO mice showed significantly increased CFUs of *K. pneumoniae* in the lung tissue and alveolar macrophages (AMs) when compared with WT mice (Fig. 1B and C showing CFU per gram lung or per 1000 AMs; $p < 0.001$, one-way ANOVA). To better understand the role of Cav1, we also investigated bacterial burdens at an early time point (8 h postinfection) (4 mice/group), and our results showed that CFUs in BAL cells and in lung homogenates were also significantly increased in C*av1* KO mice as compared with WT mice (Fig. 1D and E).

Cav1 deficiency is associated with more severe lung injury

To determine lung injury caused by *K. pneumoniae* infection, the levels of polymorphonuclear neutrophils in BAL cells and lungs from both *cav1* KO and WT mice were assayed. The proportion of neutrophils in the BAL fluid was significantly elevated in *cav1* KO mice after 24 h *K. pneumoniae* infection (Fig. 2A). As compared with WT mice, there was also increased neutrophil infiltration and interstitial edema in the lung tissue of *cav1* KO mice, while no (comparable) change was observed in controls without *K. pneumoniae* infection (Fig. 2B). We found that neutrophils started to migrate to the lung in KO mice about 4 h after infection, while no neutrophils were detected in the BAL at the beginning (<1 h). In addition, no neutrophils were observed in control mice without KP infection (data not shown). Finally, levels of myeloperoxidase (MPO) in lung were found to be significantly elevated in *cav1* KO mice compared with WT mice following infection (Fig. 2C and D, $p = 0.044$). We further determined reactive oxygen species (ROS) levels in the lungs using the H_2DCF method [16]. As shown in Fig. 2D, levels of ROS were more significantly increased in *cav1* KO mice than in WT mice ($p = 0.02$). A higher level of ROS was also observed in infected WT mice compared with the noninfection group. These data collectively suggest that more severe lung injury and oxidation occurred in *cav1* KO mice than in WT mice upon *K. pneumoniae* infection.

Cav1 deficiency alters *K. pneumonia*-induced inflammation in BAL fluid and organs

To analyze whether Cav1 deficiency impacts the inflammatory responses induced by *K. pneumonia* infection, cytokine levels in BAL fluid were assayed by ELISA at 24 h after infection. Levels of TNF-α, IL-1β, IL-6, and IL-17 were found to be significantly increased in BAL fluid from infected *cav1* KO mice as compared with levels in BAL fluid from infected WT mice, while the concentrations of IFN-γ, IL-2, IL-10, and IL-4 were not significantly altered (Fig. 3A–H). This indicates that loss of Cav1 may accelerate the proinflammatory response in mice infected by *K. pneumoniae* (Fig. 3A–H).

Since it is possible that bacterial burdens may trigger profound tissue injury and mortality, it is also necessary to analyze the cytokine levels at earlier times. We examined cytokine levels at an earlier time (8 h post-infection), and our results showed that IFN-γ, TNF-α, IL-1β, IL-6, and IL-10 were also increased in infected C*av1* KO mice as compared with levels in infected WT mice (Fig. 4A–E), indicating that Cav1 deficiency may play an important regulatory role in cytokine production in the *K. pneumonia*-infected lung. Because Cav1 has been implicated in the negative regulation of cytokines, downregulation of Cav1 may intensify proinflammatory cytokine production, contributing to disease development and intensified tissue damage.

Because IL-27p28 can broadly inhibit various cytokines from T cells including Th17 cells, we sought to further analyze the cytokine network, and quantified IL-27p28 in the lung and kidney to assess organ-specific pathology. The level of IL-27p28 was increased in both the lung and kidney of infected Cav 1 KO mice as compared with infected WT mice, whereas MIP2 (a chemokine released by macrophages) was increased only in the kidney (Fig. 4F–I). These data suggest that immunity against this infection may be related to compartmental variations in cytokine levels and may be involved in macrophages as well as T cells.

Cav1 KO mice are more susceptible to septicemia

One cause of mortality during bacterial pneumonia is its systemic dissemination into other major organs, a phenomenon known as septicemia. We assayed bacterial burdens in the liver and kidney (Fig. 4J and K). *Cav1* KO mice showed significantly increased CFUs in the liver ($p = 0.001$) and kidney ($p < 0.001$) as compared with WT mice. This result indicates that more severe dissemination occurred in *cav1* KO mice than in WT mice.

STAT5 and Akt contribute to the infectious phenotypes

We studied the regulatory mechanism underlying the susceptibility to *K. pneumoniae* infection in *cav1* KO mice. Using western blotting, we found that the GSK3β–β-catenin–Akt pathway may be involved in controlling *K. pneumoniae* infection. The protein levels of GSK3β and IL-12a, as well as phosphorylation of Akt, GSK3β, and ERK1/2, were significantly elevated in *cav1* KO mice following *K. pneumoniae* infection, while the protein levels of Akt, β-catenin, and STAT5 (also p-STAT5) were markedly downregulated (Fig. 5A and B, and densitometry analysis, Fig. 5C). Thus, the decreased levels of STAT5 and Akt, as well as increased levels of IL-6 and IL-12a, may result from the loss of Cav1's negative feedback mechanism. These data suggest that the STAT5 pathway may be downregulated by a negative signal from the GSK3β – β-catenin – Akt axis in this model. Since the early time point showed altered cytokine responses, we next evaluated relevant cell signaling proteins at 8-h postinfection. Our data (Fig. 5D and E) demonstrate that the cell signaling pattern at 8 h postinfection is also altered in *cav1* KO mice versus WT mice by infection. Importantly, the major responsive proteins (e.g. Akt, β-catenin, KC, and STAT5) at 8 h showed similar decreases, while other signaling proteins (GSK3β and IL-12a) did not display the increases seen at 24 h. These data were densitometrically analyzed as shown in Fig. 5F. Thus, the cell signaling data at early time points are in-line with the signaling results at late time points. However, as not all increases/decreases were the same at 8 and 24 h, our data also indicate that the cytokine responses may increase as the disease progresses. The expression of Akt and STAT5 was also measured in lung tissue using immunohistochemistry, which showed decreased staining for both proteins in *cav1* KO mice versus WT mice after infection (Fig. 5G, arrows indicating significant changes in fluorescent intensity between control and KO mice lungs). As previous studies show that GSK3β can destabilize β-catenin [17], we speculate that GSK3β may negatively regulate Akt or β-catenin, leading to a lowered STAT5 and dysregulated cytokine patterns. Since IL-27 has previously been shown to be associated with STAT1, we also evaluated the expression levels of STAT1, and found that there were no significant differences between control mice and KO mice (data not shown). Similar changes in β-catenin, GSK3β, and cytokine (IL-6 and IL-12a) levels were observed in lung tissue of *cav1* KO mice as assessed by immunostaining (Supporting Information Fig. 1 and 2). Importantly, as assessed by western blotting, the expression pattern of the investigated cell signaling molecules at 8 h was similar to that at the late time point.

STAT5 pathway is altered by knocking down Cav1 in MLE-12 cells

To gain insights into the impact of Cav1 on Akt-STAT5 signaling, we transfected murine alveolar epithelial MLE-12 cells with either WT *cav1* or a dominant negative (DN) *cav1*

expressing plasmid as described previously [18]. MLE-12 cells are widely used as a model for murine lung epithelial function [11]. Twenty-four hours after transfection, cells were infected with *K. pneumonia* for 1 h at 10:1 MOI and lysed in order to evaluate CFUs. As expected, decreased bacterial clearance was observed in *cav1* knockdown cells as compared with WT or vector control cells (Fig. 6A). Similarly, blocking STAT5 with a chemical inhibitor WP1066 decreased bacterial clearance, although to a lesser extent than did *cav1* DN transfection (Fig. 6A). Consistent with the in vivo data, the levels of ROS were also elevated in *cav1* knockdown cells compared with control cells following *K. pneumonia* infection (Fig. 6B, $p = 0.01$) as quantified by the H_2DCF assay and similarly increased ROS was also measured with the NBT method (Supporting Information Fig. 3). Furthermore, we determined cell survival after transfection with the *cav1* DN plasmid. As assessed by the MTT cell proliferation assay, we saw significantly decreased survival of *cav1* DN transfected cells when compared with WT cells following *K. pneumonia* infection (Supporting Information Fig. 4). These results indicate that more cell death occurred in the *cav1* knockdown cells than in WT cells challenged by *K. pneumonia*.

Importantly, mutation of Cav1 resulted in a similar increase in phospho-STAT5 while no apparent increase in total STAT5 protein was observed at 1 h (note that the tissue was obtained 24 h postinfection). Although Cav1 mutation resulted in significantly decreased β-catenin protein expression following 1 h infection, the WT plasmid transfected cells showed a much greater increase. These results are largely consistent with the data from *cav1* KO mice, indicating that Cav1 deficiency altered the expression of STAT5 and Akt. This change may contribute to the dysregulated cytokine profile, resulting in extremely high levels of IL-6 and IL-12a (Fig. 6C). To confirm the role of STAT5, a STAT5 inhibitor (WP1066) was used to pretreat the *cav1* DN cells. WP1066 has been demonstrated to inhibit the phosphorylation of STAT5, thereby blocking STAT5 signaling [19]. Perturbation of STAT5 by WP1066 significantly reduced phospho-STAT5 and downregulated IL-6 and IL-12a expression (Fig. 6D), but did not impact the expression of β-catenin, Akt, and STAT5 protein. These data support the notion that STAT5 plays a crucial regulatory role in the activation of cytokine secretion under Cav1 deficiency. In addition, Cav1 may directly influence the function of β-catenin as Cav1 DN transfection dramatically reduced its expression levels. The transfection alone did not alter cytokine levels prior to infection. The expression of IL-6 in the supernatant is also increased as seen in the cell lysate (data not shown). Collectively, these in vitro results confirm our findings derived from *cav1* KO mice indicating that the typical phenotypes for *K. pneumoniae* infection in these mice may result from a dysregulated proinflammatory response associated with altered Akt-STAT5 regulation (Fig. 7).

Discussion

We show severely impaired immunity in *cav1* KO mice after infection by *K. pneumoniae*. *cav1* KO mice exhibited a lethal phenotype including elevated bacterial burdens, severe lung injury, and increased septicemia compared with WT mice. The levels of TNF-α, IL-1β, and IL-6 were significantly increased in BAL fluid. IL-27p28 was increased both in the lung and kidney, while MIP2 was increased only in the kidney. Our studies indicate that this cytokine profile was regulated by the GSK3β–β-catenin–Akt pathway, which may impact STAT5 activity. In addition, the phagocytic ability of AMs was found to be impaired in infected animals. To our knowledge, these data are the first to reveal that Cav1 is a critical regulator for bacterial immunity against *K. pneumoniae*. As Cav1 KO mice may gradually develop respiratory complications including fibrosis in late age (12 months), the mice used for infection were younger than 4 months of age.

Recent studies using *cav1* KO mice have linked Cav1 to innate immunity against *P. aeruginosa* in lung epithelial cells [9–11]. *P. aeruginosa* utilizes lipid raft-mediated endocytosis as a means of invasion [6,20–22]. Since Cav1 is a structural protein of lipid rafts, Cav1 deficiency is thought to compromise immune function against *P. aeruginosa* [1,9,10]. To better characterize the role of Cav1 in bacterial infections, we studied the immune response of cav1 KO mice against another bacterium, *K. pneumoniae*. As this bacterium has not been documented to invade host cells via lipid rafts, this model may complement previous studies on Cav1's immunity. *cav1* KO mice exhibited a severe outcome following *K. pneumoniae* infection compared with WT mice: elevated bacterial numbers, exacerbated lung injury, and severe septicemia. These results are consistent with previous findings [9], wherein *P. aeruginosa*-induced pneumonia developed into a systemic bacterial infection in *cav1* KO mice. Along the same lines, Lisanti et al. reported that *cav1* KO mice displayed decreased survival rates when intravenously challenged with *S. Typhimurium* [8]. Therefore, our current data support the growing consensus that Cav1 fulfills a crucial function in resistance to invasive pathogens.

TNF-α and IL-1β are two potent proinflammatory cytokines. Our results show that their contributions to the proinflammatory response to *K. pneumonia* intensified under Cav1 deficiency. Both of these cytokines also share a wide range of biological activities, including neutrophil penetration [23]. Neutralization of TNF-α activity impairs host defense during *Klebsiella* pneumonia and results in increased bacterial burdens and mortality [24]. This was similarly seen in *P. aeruginosa*-infected *cav1* KO mice [9]. Interestingly, IL-6 was also elevated not only in *cav1* KO mice challenged with *K. pneumoniae*, but also in those exposed to *P. aeruginosa*. IL-6 plays disparate roles in inflammatory responses during bacterial infections [25]. IL-6 protects the host from death following *K. pneumoniae* infection; however, IL-6 neutralizing antibodies improve survival in polymicrobial septic peritonitis [26]. Since IL-17R-deficient mice were shown to be more susceptible to *K. pneumonia* infection [27], we measured IL-17 levels and found an increase in *cav1* KO mice compared with WT mice lungs. In fact, the susceptibility of IL-17-deficient mice to *K. pneumoniae* has been directly associated with delayed neutrophil recruitment and reduced G-CSF [28]. IL-17 has also been documented to induce secretion of TNFα, IL-1β, and IL-6 [29]. The proinflammatory response to *K. pneumoniae* may not improve survival rates, but it aggravates existing disease conditions as shown in *cav1* KO mice infected with *P. aeruginosa* [9,11]. Despite the elevated levels of TNF-α, IL-1β, IL-6, and IL-17 in BAL fluid, the overall survival of *cav1* KO mice with *K. pneumoniae* infection deteriorated rapidly. Interestingly, IL-27p28, a novel cytokine, was also increased in infected *cav1* KO mice. p28, a subunit of IL-27, has broad inhibitory effects on Th1, Th2, and Th17 subsets as well as the expansion of regulatory T cells [30]. Hence, we propose that the elevated IL-27 may provide a passive regulatory mechanism during acute infection.

Given that MIP2 is a chemokine primarily produced by macrophages, our finding that MIP2 levels were not elevated in the lung indicates an impaired alveolar macrophage population. This in turn suggests that distinct compartmental immunity occurs in *K. pneumoniae* infection [31]. In addition, the phagocytic ability of AMs was found to be downregulated in *K. pneumoniae*-infected *cav1* KO mice (data not shown).

It has been suggested that Cav1 is an immune-modulatory effector on cytokine production through the MKK3/p38 MAPK pathway [32]. We found that ERK1/2 was activated in *cav1* KO mice. We also noted a decreased TLR-4 response that was previously linked to gram-negative bacteria, suggesting a troublesome lack of innate immunity in *cav1* KO mice. We also observed that GSK3β–β-catenin–Akt pathway may be involved in this infection, with both Akt and β-catenin being downregulated by Cav1 deficiency. By contrast, GSK3β expression and phosphorylation are significantly increased following loss of Cav1. This is

consistent with the previous studies that show that GSK3β can destabilize β-catenin [17]. Although Akt is usually an upstream signal for GSK3β [33,34], in this case the Akt changes may result from the effects of GSK3β [35]. Our data strongly support the GSK3β–β-catenin–Akt axis, which may also influence the STAT5 signaling pathway. Importantly, we found that proinflammatory cytokines may be dysregulated by a decreased STAT5. STAT5 normally stimulates an inflammatory response during bacterial infection [36]. Park et al. [37] have shown that Cav1 is a negative regulator of JAK2/STAT5a signaling in the mammary gland. This negative regulation may occur through direct molecular interaction owing to structural homology between Cav1 and SOCS-1 or SOCS3 [38]. Our data suggest that the GSK3β–β-catenin–Akt axis may be related to a decreased STAT5 profile, making a connection from Cav1 deficiency to the exacerbated inflammatory response.

Although the above research begins to hint at some important answers, it is not known why decreased STAT5 functionality leads to an increased proinflammatory cytokine profile. Previous reports have shown that Akt can connect to STAT5 and regulate neuroprotective activity or cancer development [39]. However, little is known as to the specific functions of the GSK3β–β-catenin–Akt axis in bacterial infection. We hypothesized that decreased STAT5 may be regulated by changes in GSK3β or from the loss of Akt/β-catenin activity (at middle or late phases of infection), since our in vitro assays indicated an increase in pSTAT5 at early phases of infection. Following PIP_3 and PI3K activation, Akt activation is required to regulate apoptosis against LPS or other oxidants [40], which could also be associated with a heightened inflammatory response. Akt is negatively regulated under Cav1 deficiency, while GSK3β is upregulated. As feedback, Akt can inhibit GSK3β, thereby reducing the negative regulation of GSK3β in cellular processes. We assumed that an excessive inflammatory response and inefficient apoptotic clearance of dead cells lead to severe lung injury. Thus, an interaction between Akt and Cav1 may broadly impact the cytokine production and disease process. Downregulation of Akt and STAT5 was initiated to counteract the loss of Cav1, but failed to eradicate the invading bugs. As a result, IL-6 and related cytokines could not be properly controlled by feedback signaling, contributing to the severe infection seen in *cav1* KO mice.

In summary, our studies illustrate a typical phenotype in *cav1* KO mice following *K. pneumoniae* infection, characterized by increased bacterial burdens in the lung, decreased survival, severe lung injury, and increased inflammatory response. Furthermore, the increased impairment of the immune system in these KO mice is at least in part attributed to a regulatory function of the STAT5 pathway, which is, in turn, influenced by a GSK3β–β-catenin–Akt axis. Our studies have also characterized a novel role of Cav1 in infection resistance and explored its involvement with the Akt-STAT5 cross-talk, whose underlying mechanisms warrant further study. More specifically, our data may shed light on the pathogenesis of *K. pneumoniae* infection and suggest a novel therapeutic target.

Materials and methods

Animals

Cav1 KO and WT mice (B6129SF2/J) mice were obtained from the Jackson Laboratory (Bar Harbor, ME). Mice were housed and bred in the Biomedical Research Facility at University of North Dakota. All the animal procedures have been approved by the UND IACUC committee.

Bacteria preparation and induction of *K. pneumoniae* infection in mice

K. pneumoniae (ATCC 43816 serotype II) was provided by Dr. V. Miller (Washington University, St. Louis) [41]. Bacteria were grown overnight in LB broth at 37°C with

shaking. The bacteria were pelleted by centrifugation at 5000 × *g*. We then anesthetized mice with 45 mg/kg ketamine and intranasally instilled 2×10^5 colony-forming units (CFUs) of *K. pneumoniae* in PBS (50 μl).

Cell estimation in BAL and isolation of AMs

BAL was performed 5 times with 1.0 mL volumes of lavage fluid, while the first 0.5 mL was saved separately for cytokine detection. A cell smear was made from the BAL fluid and stained with HEMA-3 (Fisher, Rockford, IL) for cell differential counting. AMs were collected from the BAL fluid precipitate after centrifuging at 2000 × *g* for 5 min at 4°C and cultivated in RPMI 1640 medium supplemented with 10% newborn calf serum and penicillin/streptomycin in a 5% CO_2 incubator.

Histological studies

After BAL procedures, the lung, liver, and kidneys were aseptically harvested for homogenization or fixed in 10% formalin or OCT [42]. For evaluating bacterial burdens in BAL AMs, and lung tissue, BAL was performed to get rid of the free bacteria. Homogenization of lung tissue was done using liquid nitrogen and samples kept on dry ice before dissolving in RIPA buffer for western blotting analysis or in PBS for CFU and superoxide analysis. For western blotting, the samples were sonicated for three times at 10 s each. Histology slides were made after formalin fixation, and stained with the standard hematoxylin-eosin method [43]. For immunohistochemistry assays, we performed OCT fixation and cryosection and stained the slides using the methods described previously [44].

Colony forming units

AMs were resuspended in lysis solution. Lung or other tissues were homogenized by pestle/mortar in liquid nitrogen and followed by brief sonication. AMs from BAL fluid or homogenized tissues of the lung, liver, and kidneys were spread on LB plates to enumerate the bacteria that have invaded into AMs or tissues. Free bacteria were killed with polymycin B (200 μg/mL) for 1 h and washed away by lavage. Selected unlavaged samples were also saved and assessed to evaluate the differences in cell signaling. The plates were cultured in a 37°C incubator for 18 h, and bacterial colonies were counted [22]. Triplicates were done for each sample and control.

Cytokine determination

Cytokine concentrations in BAL fluids (the first 0.5 mL lavage solution) or tissues were measured by standard ELISA kits according to the manufacturer's instructions (eBioscience company, San Diego, CA) [45]. To overcome detection limits (5 pg/mL), we have only used the initial 0.5 mL of lavage solution to determining cytokine concentrations.

Western blotting analysis

Mouse monoclonal Abs against Cav1, Akt, phospho-ERK, STAT5, IL-6, IFNγ, and rabbit polyclonal Abs against KC, GSK3β, β-catenin, IL-12a, and goat polyclonal Abs against TNFα were from Santa Cruz Biotechnology (Santa Cruz, CA). Rabbit monoclonal Ab against GAPDH was obtained from Cell Signaling Technology (Danvers, MA). Western blotting of lung homogenates was performed as described previously [46,47].

RT-PCR analysis

RNA was extracted from lung homogenates and cells with Trizol (Invitrogen Life Technologies, Carlsbad, CA) according to the manufacturer's instructions. Reverse transcription was performed using 1.5 μg of RNA and cDNA was amplified using gene-specific primers [48,49]. The results were normalized with GAPDH.

MPO assay

MPO assay was performed as described previously (15). Samples were homogenized in 50 mM hexadecyltrimethylammonium bromide (HTAB) and assayed as previously described [45,50].

Dihydrodichlorofluorescein diacetate (H_2DCF) assay for superoxide production

H_2DCF dye (Molecular Probes) does not normally fluoresce under resting conditions, but emits green fluorescence upon reaction with superoxide inside cells. Cells were treated as above and equal amounts of dye added [16].

3-(4,5-dimethylthiazol-2-yl)-2,5-dimethyltetrazolium bromide (MTT) assay

This assay measures color change of MTT upon reduction by enzymes to assess the viability of cells. After infection of MLE-12 cells with *K. pneumoniae*, MTT dye was added at a final concentration of 1 μg/mL as described previously [47].

Transfection of MLE-12 cells

We used LipofectAmine2000 to transfect cells at 60% confluency and achieved high efficiency in transfection [22,51]. The yellow fluorescent protein (YFP)-Cav-1, YFP-Cav-1Δ51-169 dominant negative (DN) plasmids were generated as described previously [18]. MLE-12 cells were infected with *K. pneumoniae* at MOI 10:1 for 1 h and the free bacteria were removed by washing three times with PBS. The surface bacteria were killed by incubation with 100 μg/mL polymyxin B for 1 h and intracellular bacteria were enumerated to determine CFU. Transfection with *cav1* DN plasmid did not affect survival of MLE-12 cells prior to incubation with *K. pneumoniae*. WP1066 (a novel STAT5 inhibitor from Sigma) was dissolved in 1% DMSO solution and used at a final concentration of 2 μM in culture medium. No adverse effect of the vehicle control was observed in the assays.

Statistical analyses

The differences in outcomes between *cav1* KO and WT control animals after *K. pneumoniae* infection were calculated by Kaplan–Meier survival curve comparisons, and the *p* values were derived from a log-rank test. Most experiments were performed three times in triplicate. Comparison of experimental groups with controls was done with one-way ANOVA (Tukey's post-hoc) [16,52].

Supplementary Material

Refer to Web version on PubMed Central for supplementary material.

Acknowledgments

This project was supported by NIH ES014690, Flight Attendant Medical Research Institute (FAMRI, 103007), and American Heart Association Scientist Development Grant (MW); and by NIH 5R01HL092905-04 and 3R01HL092905-02S1 (HG). We thank S. Rolling of UND imaging core for help with confocal imaging.

Abbreviations

AM	alveolar macrophage
BAL	bronchoalveolar lavage
Cav-1	caveolin-1
DN	dominant negative

H_2DCF	dihydrodichlorofluorescein diacetate
JAK	Janus kinase
MPO	myeloperoxidase
SOCS	suppressors of cytokine signaling
TBARS	thiobarbituric acid reactive substance

References

1. Anderson RG. The caveolae membrane system. Annu. Rev. Biochem. 1998; 67:199–225. [PubMed: 9759488]
2. Shin JS, Abraham SN. Cell biology. Caveolae – not just craters in the cellular landscape. Science. 2001; 293:1447–1448. [PubMed: 11520975]
3. Pelkmans L, Kartenbeck J, Helenius A. Caveolar endocytosis of simian virus 40 reveals a new two-step vesicular-transport pathway to the ER. Nat. Cell Biol. 2001; 3:473–483. [PubMed: 11331875]
4. Moriyama T, Marquez JP, Wakatsuki T, Sorokin A. Caveolar endocytosis is critical for BK virus infection of human renal proximal tubular epithelial cells. J. Virol. 2007; 81:8552–8862. [PubMed: 17553887]
5. Wang XM, Nadeau PE, Lo YT, Mergia A. Caveolin-1 modulates HIV-1 envelope-induced bystander apoptosis through gp41. J. Virol. 2010; 84:6515–6526. [PubMed: 20392844]
6. Zaas D, Duncan M, Li G, Wright JR, Abraham SN. Pseudomonas invasion of type I pneumocytes is dependent on the expression and phosphorylation of caveolin-2. J. Biol. Chem. 2005; 280:4864–4872. [PubMed: 15545264]
7. Garrean S, Gao XP, Brovkovych V, Shimizu J, Zhao YY, Vogel SM, Malik AB. Caveolin-1 regulates NF-kappaB activation and lung inflammatory response to sepsis induced by lipopolysaccharide. J. Immunol. 2006; 177:4853–4860. [PubMed: 16982927]
8. Medina FA, de Almeida CJ, Dew E, Li J, Bonuccelli G, Williams TM, Cohen AW, et al. Caveolin-1-deficient mice show defects in innate immunity and inflammatory immune response during Salmonella enterica serovar Typhimurium infection. Infect Immun. 2006; 74:6665–6674. [PubMed: 16982844]
9. Gadjeva M, Paradis-Bleau C, Priebe GP, Fichorova R, Pier GB. Caveolin-1 modifies the immunity to *Pseudomonas aeruginosa*. J. Immunol. 2010; 184:296–302. [PubMed: 19949109]
10. Zaas DW, Swan ZD, Brown BJ, Li G, Randell SH, Degan S, Sunday ME, et al. Counteracting signaling activities in lipid rafts associated with the invasion of lung epithelial cells by *Pseudomonas aeruginosa*. J. Biol. Chem. 2009; 284:9955–9964. [PubMed: 19211560]
11. Yuan K, Huang C, Fox J, Gaid M, Weaver A, Li GP, Singh BB, et al. Elevated inflammatory response in Caveolin-1 deficient mice with *P. aeruginosa* infection is mediated by STAT3 and NF-{kappa}B. J. Biol. Chem. 2011; 286:21814–21825. [PubMed: 21515682]
12. Shankar-Sinha S, Valencia GA, Janes BK, Rosenberg JK, Whitfield C, Bender RA, Standiford TJ, et al. The *Klebsiella pneumoniae* O antigen contributes to bacteremia and lethality during murine pneumonia. Infect Immun. 2004; 72:1423–1430. [PubMed: 14977947]
13. Korvick JA, Bryan CS, Farber B, Beam TRJ, Schenfeld L, Muder RR, Weinbaum D, et al. Prospective observational study of *Klebsiella bacteremia* in 230 patients: outcome for antibiotic combinations versus monotherapy. Antimicrob. Agents Chemother. 1992; 36:2639–2644. [PubMed: 1482131]
14. Geffen Y, Finkelstein R, Oren I, Shalaginov R, Tavleva I, Sprecher H. Changing epidemiology of carbapenem-resistant *Enterobacteriaceae carriage* during an outbreak of carbapenem-resistant *Klebsiella pneumoniae*. J. Hosp. Infect. 2010; 76:355–356. [PubMed: 20965609]
15. Cai S, Batra S, Lira SA, Kolls JK, Jeyaseelan S. CXCL1 regulates pulmonary host defense to Klebsiella infection via CXCL2, CXCL5, NF-kappaB, and MAPKs. J. Immunol. 2010; 185:6214–6225. [PubMed: 20937845]

16. Wu M, Huang H, Zhang W, Kannan S, Weaver A, Mckibben M, Herington D, et al. Host DNA repair proteins in response to *P. aeruginosa* in lung epithelial cells and in mice. Infect Immun. 2011; 79:75–87. [PubMed: 20956573]
17. Dao MA, Creer MH, Nolta JA, Verfaillie CM. Biology of umbilical cord blood progenitors in bone marrow niches. Blood. 2007; 110:74–81. [PubMed: 17371947]
18. Brazer SC, Singh BB, Liu X, Swaim W, Ambudkar IS. Caveolin-1 contributes to assembly of store-operated Ca2+ influx channels by regulating plasma membrane localization of TRPC1. J. Biol. Chem. 2003; 278:27208–27215. [PubMed: 12732636]
19. Kong LY, Wei J, Sharma AK, Barr J, Abou-Ghazal MK, Fokt I, Weinberg J, et al. A novel phosphorylated STAT3 inhibitor enhances T cell cytotoxicity against melanoma through inhibition of regulatory T cells. Cancer Immunol. Immunother. 2009; 58:1023–1032. [PubMed: 19002459]
20. Soong G, Reddy B, Sokol S, Adamo R, Prince A. TLR2 is mobilized into an apical lipid raft receptor complex to signal infection in airway epithelial cells. J. Clin. Invest. 2004; 113:1482–1489. [PubMed: 15146246]
21. Kowalski MP, Pier GB. Localization of cystic fibrosis transmembrane conductance regulator to lipid rafts of epithelial cells is required for *Pseudomonas aeruginosa*-induced cellular activation. J. Immunol. 2004; 172:418–425. [PubMed: 14688350]
22. Kannan S, Audet A, Knittel J, Mullegama S, Gao GF, Wu M. Src kinase Lyn is crucial for *Pseudomonas aeruginosa* internalization into lung cells. Eur. J. Immunol. 2006; 36:1739–1752. [PubMed: 16791881]
23. Lepper PM, Möricke A, Held TK, Schneider EM, Trautmann M. K-antigen-specific, but not O-antigen-specific natural human serum antibodies promote phagocytosis of *Klebsiella pneumoniae*. FEMS Immunol. Med. Microbiol. 2003; 35:93–98. [PubMed: 12628543]
24. Laichalk LL, Kunkel SL, Strieter RM, Danforth JM, Bailie MB, Standiford TJ. Tumor necrosis factor mediates lung antibacterial host defense in murine *Klebsiella pneumonia*. Infect Immun. 1996; 64:5211–5218. [PubMed: 8945568]
25. Akira S, Taga T, Kishimoto T. Interleukin-6 in biology and medicine. Adv. Immunol. 1993; 54:1–78. [PubMed: 8379461]
26. Riedemann NC, Neff TA, Guo RF, Bernacki KD, Laudes IJ, Sarma JV, Lambris JD, et al. Protective effects of IL-6 blockade in sepsis are linked to reduced C5a receptor expression. J. Immunol. 2003; 170:503–507. [PubMed: 12496437]
27. Ye P, Rodriguez FH, Kanaly S, Stocking KL, Schurr J, Schwarzenberger P, Oliver P, et al. Requirement of interleukin 17 receptor signaling for lung CXC chemokine and granulocyte colony-stimulating factor expression, neutrophil recruitment, and host defense. J. Exp. Med. 2001; 194:519–527. [PubMed: 11514607]
28. Curtis MM, Way SS. Interleukin-17 in host defence against bacterial, mycobacterial and fungal pathogens. Immunology. 2009; 126:177–185. [PubMed: 19125888]
29. Jovanovic DV, Di Battista JA, Martel-Pelletier J, Jolicoeur FC, He Y, Zhang M, Mineau F, Pelletier JP. IL-17 stimulates the production and expression of proinflammatory cytokines, IL-beta and TNF-alpha, by human macrophages. J. Immunol. 1998; 160:3513–3521. [PubMed: 9531313]
30. Stumhofer JS, Hunter CA. Advances in understanding the antiinflammatory properties of IL-27. Immunol. Lett. 2008; 117:123–130. [PubMed: 18378322]
31. Hunninghake GW, Crystal RG. Pulmonary sarcoidosis: a disorder mediated by excess helper T-lymphocyte activity at sites of disease activity. New Engl. J. Med. 1981; 305:429–434. [PubMed: 6454846]
32. Wang XM, Kim HP, Song R, Choi AM. Caveolin-1 confers antiinflammatory effects in murine macrophages via the MKK3/p38 MAPK pathway. Am. J. Respir Cell Mol. Biol. 2006; 34:434–442. [PubMed: 16357362]
33. Zhu QS, Xia L, Mills GB, Lowell CA, Touw IP, Corey SJ. G-CSF induced reactive oxygen species involves Lyn-PI3-kinase-Akt and contributes to myeloid cell growth. Blood. 2006; 107:1847–1856. [PubMed: 16282349]
34. Liang J, Slingerland JM. Multiple roles of the PI3K/PKB (Akt) pathway in cell cycle progression. Cell Cycle. 2003; 2:339–345. [PubMed: 12851486]

35. Di Santo A, Amore C, Dell'Elba G, Manarini S, Evangelista V. Glycogen synthase kinase-3 negatively regulates tissue factor expression in monocytes interacting with activated platelets. J. Thromb. Haemost. 2011; 9:1029–1039. [PubMed: 21320285]
36. Ivashkiv LB. STAT activation during viral infection in vivo: where's the interferon? Cell Host Microbe. 2010; 8:132–135. [PubMed: 20709291]
37. Park DS, Lee H, Frank PG, Razani B, Nguyen AV, Parlow AF, Russell RG, et al. Caveolin-1-deficient mice show accelerated mammary gland development during pregnancy, premature lactation, and hyperactivation of the Jak-2/STAT5a signaling cascade. Mol. Biol. Cell. 2002; 13:3416–3430. [PubMed: 12388746]
38. Norkina O, Dolganiuc A, Catalano D, Kodys K, Mandrekar P, Syed A, Efros M, et al. Acute alcohol intake induces SOCS1 and SOCS3 and inhibits cytokine-induced STAT1 and STAT3 signaling in human monocytes. Alcohol Clin. Exp. Res. 2008; 32:1565–1573. [PubMed: 18616672]
39. Byts N, Samoylenko A, Fasshauer T, Ivanisevic M, Hennighausen L, Ehrenreich H, Sirén AL. Essential role for Stat5 in the neurotrophic but not in the neuroprotective effect of erythropoietin. Cell Death Differ. 2008; 15:783–792. [PubMed: 18259195]
40. Xing J, Zhang Z, Mao H, Schnellmann RG, Zhuang S. Src regulates cell cycle protein expression and renal epithelial cell proliferation via PI3K/Akt signaling-dependent and -independent mechanisms. Am. J. Physiol. Renal Physiol. 2008; 295:F145–152. [PubMed: 18434386]
41. Lawlor MS, Hsu J, Rick PD, Miller VL. Identification of *Klebsiella pneumoniae* virulence determinants using an intranasal infection model. Mol. Microbiol. 2005; 58:1054–1073. [PubMed: 16262790]
42. Wu M, Pasula R, Smith PA, Martin WJ II. Mapping alveolar binding sites in vivo using phage display peptide libraries. Gene Ther. 2003; 10:1429–1436. [PubMed: 12900757]
43. Wu M, Hussain S, He HY, Pasula R, Smith PA, Martin WJ II. Genetically engineered macrophages expressing IFN-γ restore alveolar immune function in *SCID* mice. Proc. Natl. Acad Sci. USA. 2001; 98:14589–14594. [PubMed: 11724936]
44. Kannan S, Audet A, Huang H, Chen LJ, Wu M. Cholesterolrich membrane rafts and lyn are involved in phagocytosis during *Pseudomonas aeruginosa* infection. J. Immunol. 2008; 180:2396–2408. [PubMed: 18250449]
45. Kannan S, Huang H, Seeger D, Audet A, Chen Y, Huang C, Gao H, et al. Alveolar epithelial type II cells activate alveolar macrophages and mitigate *P. aeruginosa* infection. Plos One. 2009; 4:e4891. [PubMed: 19305493]
46. Wu M, Stockley PG, Martin WJ II. An improved Western blotting effectively reduces the background. Electrophoresis. 2002; 23:2373–2376. [PubMed: 12210190]
47. Wu M, Brown WL, Stockley PG. Cell-specific delivery of bacteriophage-encapsidated ricin A chain. Bioconjugate Chem. 1995; 6:587–595.
48. Wu M, Harvey KA, Ruzmetov N, Welch ZR, Sech L, Jackson K, Stillwell W, et al. Omega-3 polyunsatuated fatty acids attenuate breast cancer growth through activation of a sphingomyelinase-mediated pathway. Int. J. Cancer. 2005; 117:340–348. [PubMed: 15900589]
49. Wu M, He Y, Xu Y, Kobune M, Kelley MR, Martin WJ II. Protection of human lung cells against hyperoxia using the DNA base excision repair genes hOgg1 and Fpg. Am. J. Respir. Crit. Care Med. 2002; 166:192–199. [PubMed: 12119232]
50. Wu M, Audet A, Cusic J, Seeger D, Cochran R, Ghribi O. Broad DNA repair responses in neural injury are associated with activation of the IL-6 pathway in cholesterol-fed rabbits. J. Neurochem. 2009; 111:1011–1021. [PubMed: 19765189]
51. Kannan S, Pang H, Foster D, Rao Z, Wu M. Human 8-oxoguanine DNA glycosylase links MAPK activation to resistance to hyperoxia in lung epithelial cells. Cell Death Differ. 2006; 13:311–323. [PubMed: 16052235]
52. Wu M, Kelley MR, Hansen WK, Martin WJ II. Reduction of BCNU toxicity to lung cells by high-level expression of O^6-methylguanine-DNA methyltransferease. Am. J. Physiol. Lung Cell Mol. Physiol. 2001; 280:L755–L761. [PubMed: 11238017]

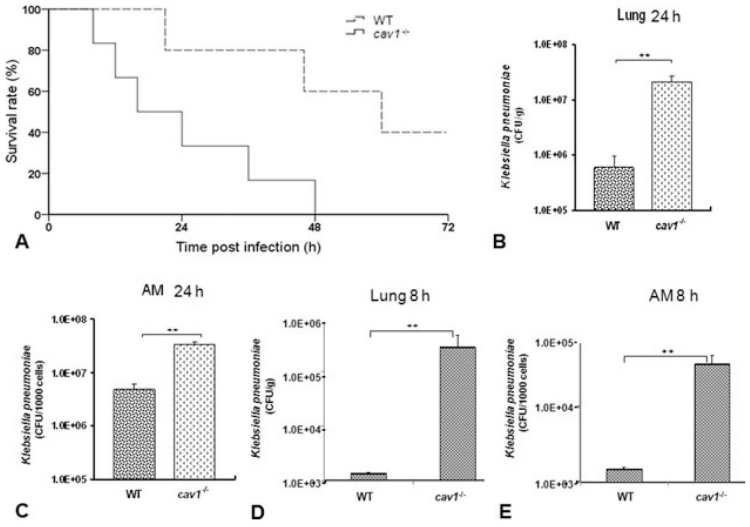

Figure 1.

Decreased survival rates and increased bacterial burdens in *cav1* KO mice following *K. pneumoniae* infection. *Cav1* KO mice ($n = 6$) and WT mice ($n = 5$) were intranasally infected with 2×10^5 CFU/mouse of *K. pneumonia*. (A) Survival was determined over time. Survival is represented by Kaplan–Meier survival curves ($p = 0.029$, 95% confidence interval: 11.7– 36.3, log-rank test). (B–E) Moribund *cav1* KO mice (6 mice) and WT mice (5 mice) were euthanized for assessment of histological and biochemical alterations. (B and D) Lungs were aseptically removed and homogenized in PBS for analysis of bacterial burden at either 8 or 24-h postinfection. The same quantity of tissue was evaluated and the data are expressed as CFU/g tissue. (C and E) AMs were derived from BALF and lysed in PBS at either 8 or 24-h postinfection. Equal numbers of AMs were used to assess bacterial burdens. Data are shown as mean + SEM ($n = 5$ per group) and are representative of three experiments. $^{++}$ $p < 0.001$ by one-way ANOVA.

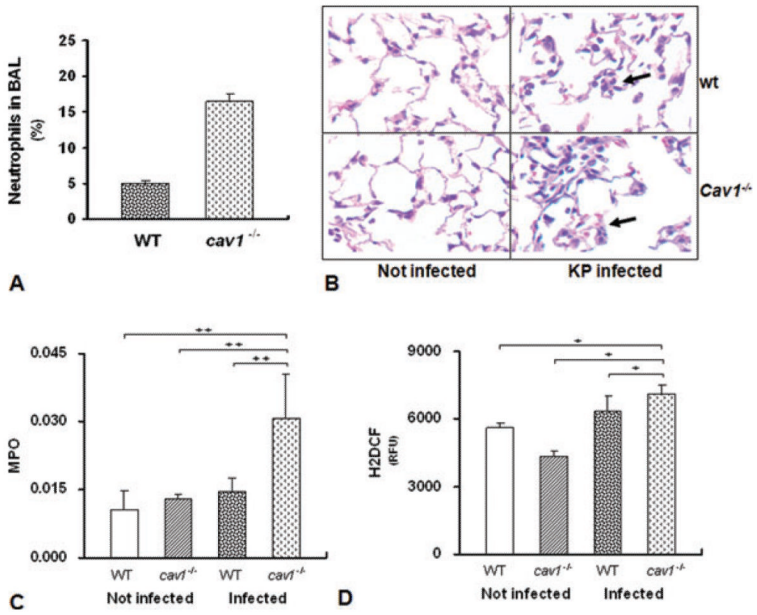

Figure 2.

Severe lung injury in *cav1* KO mice. WT and cav1 KO mice ($n = 5$ per group) were infected with 2×10^5 CFU/mouse *K. pneumoniae* for 24 h. (A) BALF was isolated and the percentage of neutrophils in total nucleated cells determined. (B) The lungs were fixed in formalin and sections were analyzed by H&E staining. One representative image of three experiments is shown. The arrows show regions of inflammation. (C) MPO levels were assessed in lung homogenates by HTAB. (D) ROS levels were assessed in lung homogenates by an H_2DCF method. (A, C, and E) Data are shown as mean + SEM ($n = 5$ per group). $^{+}$ $p = 0.044$, $^{++}$ $p = 0.02$ by one-way ANOVA.

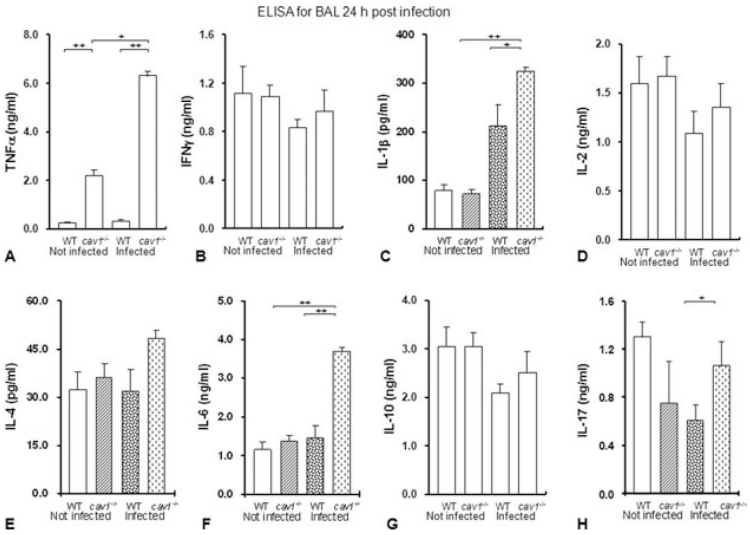

Figure 3.

Cav1 deficiency altered the inflammatory responses to *K. pneumoniae*. (A–H) ice ($n = 5$ per group) were infected with 2×10^5 CFU/mouse *K. pneumoniae* for 24 h and BALF was aseptically obtained. The cytokine profiles in BAL were assayed by ELISA. Data are shown as mean + SEM and are representative of three experiments. $^{+}$ $p < 0.05$, $^{++}$ $p < 0.01$ by one-way ANOVA.

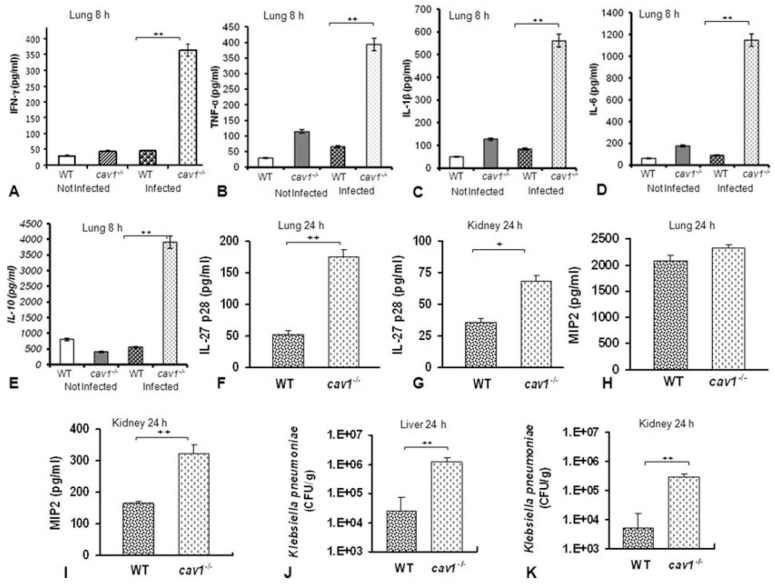

Figure 4.

Cav1 deficiency altered the inflammatory response to *K. pneumoniae* at early times and in different organs. WT mice and *cav1* KO mice (5 in each group) were infected with 2×10^5 CFU/mouse *K. pneumoniae* for (A–E) 8 h and (F–K) 24 h and the indicated organs were aseptically removed. (A–I) Cytokine/chemokine levels and (J and K) bacterial burden were evaluated. Data are shown as mean + SEM ($n = 5$ per group) and are representative of three experiments, $^{+}$ $p < 0.01$, $^{++}$ $p < 0.001$, one-way ANOVA.

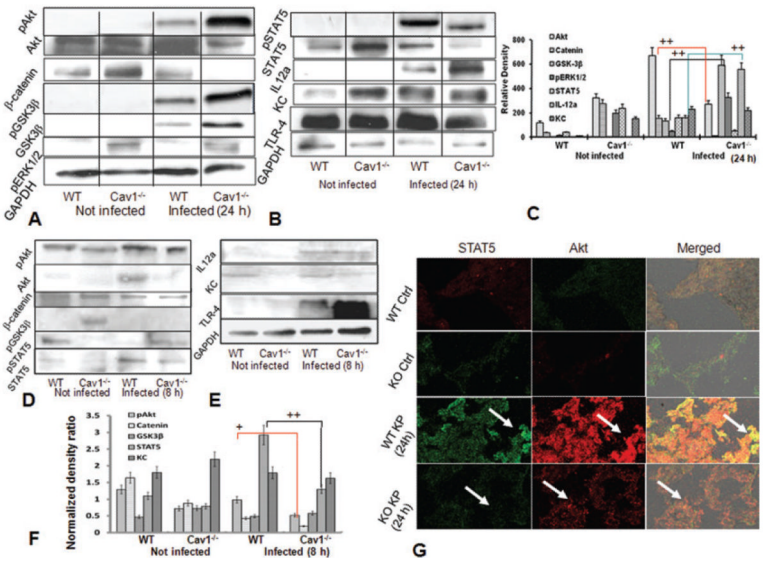

Figure 5.

Altered cellular signaling pathways in the lung with Cav1 deficiency. Mice were infected with 2×10^5 control CFU/mouse *K. pneumoniae* or sham ($n = 5$). (A and B) Lung tissues were lysed and STAT5, Akt, β-catenin, GSK3β, IL12a, and phospho-ERK1/2 levels determined by western blotting 24 h after infection. Representative blots of three experiments are shown. GAPDH serves as the loading control. (C) Densitometry quantification of the western blotting gel data presented in (A and B) using Quantity one software. Data are shown as mean + SEM; one-way ANOVA, ($n = 5$ per group) and are representative of three experiments $^{+}\ p < 0.05$, $^{++}\ p < 0.01$. (D and E) Lung tissues were lysed and the levels of the indicated molecules determined by western blotting 8 h postinfection ($n = 5$) by western blot analysis. (F) Densitometry quantification of the western blotting gel data presented in (D and E). (G) Immunohistochemistry with specific antibodies of lung tissue of *cav1* KO mice and WT mice ($n = 5$ per group) before and after infection with *K. pneumoniae* for 24 h. Arrows indicate significant changes in fluorescent intensity between control and KO mice lungs. Data are representative of three experiments.

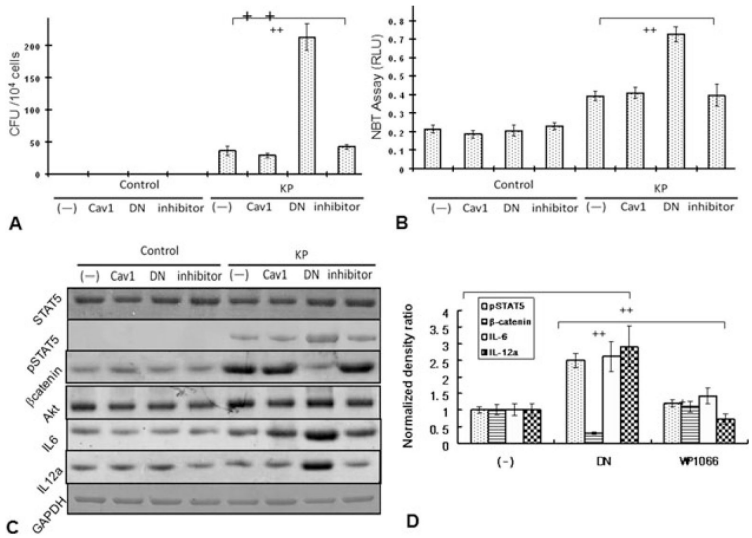

Figure 6.

MLE-12 cells expressing a dominant negative mutant *Cav1* displayed an activated STAT5 pathway following *K. pneumoniae* infection. MLE-12 cells were either transfected with *cav1* DN or *cav1* WT plasmids or treated with 2 μM STAT5 inhibitor WC1066. After 24 h, the cells were infected with *K. pneumoniae* at 10:1 MOI for 1 h and surface bacteria were killed by incubating with polymyxin B for 1 h or left uninfected. (A) Bacterial burden determined as CFUs. (B) ROS levels were determined by an H_2DCF assay. (C) Expression of the indicated molecules was determined by western blotting. GAPDH serves as the loading control. (D) Densitometry quantification of western blotting gel data presented in (C) using Quantity one software (one-way ANOVA (Tukey's post-hoc), $^{++}$ $p < 0.001$). Data are (E) representative or shown (A, B, and D) as mean ± SEM of replicates of three representative experiments.

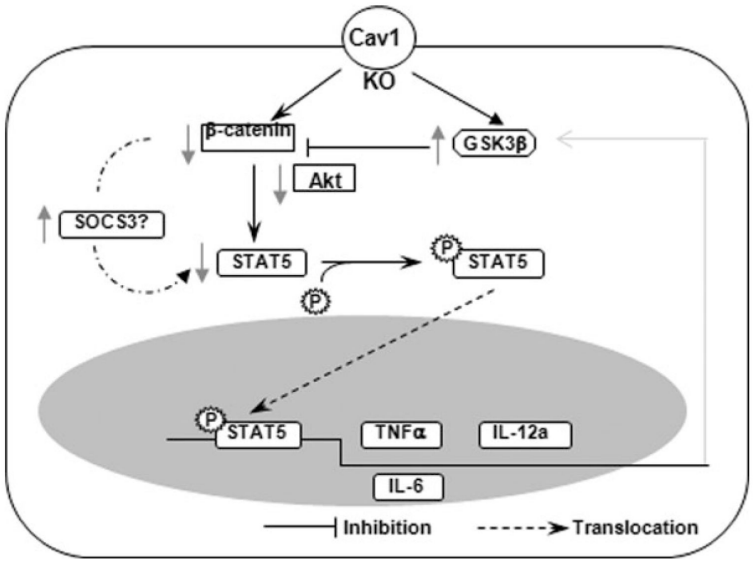

Figure 7.

Schematic diagram describing the proposed GSK3β–β-catenin–Akt axis involved in the dysregulated proinflammatory response. Cav1 knockout decreases β–catenin while increases GSK-3β expression, resulting in a decrease in Akt levels. This also downregulates STAT5 with and leads to decreased nuclear translocation, which may impact on production of cytokines such as TNF-α, IL-12a and IL-6, and infection outcome.